Composites Part B 161 (2019) 483–489

Contents lists available at ScienceDirect

Composites Part B

journal homepage: www.elsevier.com/locate/compositesb

Rheological properties of cellulose nanocrystals engineered polylactic acid nanocomposites

Jamileh Shojaeiarani[a,*], Dilpreet S. Bajwa[a], Nicole M. Stark[b], Sreekala G. Bajwa[c]

[a] Mechanical Engineering Department, North Dakota State University, Fargo, ND, 58102, United States
[b] U.S. Forest Service, Forest Products Laboratory, Madison, WI, 53726-2398, United States
[c] Agricultural and Biosystems Engineering Department, North Dakota State University, Fargo, ND, 58102, United States

ARTICLE INFO

Keywords:
Poly(lactic acid)
Cellulose nanocrystals
Masterbatch
Molecular structure
Rheological properties
Thermal stability

ABSTRACT

Ecofriendly materials such as polylactic acid (PLA) and cellulose nanocrystals (CNCs) are widely sought as potential substitute for petrochemical-based plastics. Uniform dispersion of cellulose nanocrystals in polymer matrices has inhibited their wide-spread application. In this study the influence of masterbatch preparation techniques on molecular structure, melt strength, rheological and dynamic mechanical properties of nanocomposite were systematically analyzed. Film casting and spin-coating methods were used to prepare masterbatches. Nanocomposites were obtained by masterbatch dilution via melt compounding followed by injection molding process. The higher molecular weight and lower molecular number were observed in spin-coated samples in comparison with film cast nanocomposites. The spin-coated nanocomposites exhibited higher storage modulus than film cast samples in the glassy state. However, tan δ curves exhibited higher peak value in spin-coated nanocomposites, which were in good agreement with higher dispersity index of spin-coated samples. The complex viscosity of PLA and nanocomposites exhibited non-Newtonian behavior at a low shear rate, followed by shear thinning phenomenon. The spin-coated nanocomposites demonstrated higher complex viscosity than film cast samples, which was attributed to higher molecular weight in spin-coated samples. The shear-thinning tendency in spin-coated samples was higher than film cast nanocomposites.

1. Introduction

The growing concern over ecologically friendly materials is pushing the academia and industries to seek versatile and bio-based materials for various applications. Biopolymers are considered as convenient substitutes for synthetic plastics and have received a substantial attention owing to their advantages over traditional and petroleum-based analogs. Among various biodegradable polymers, PLA which is derived from renewable resources such as sugar beet, and maize has received considerable attention as a promising polymer for packaging applications [1]. However, PLA application is still limited as a result of some inherent drawbacks like low thermal stability and low melt strength [2]. The melt strength of polymers indicates the chain resistance to untangling under shear strain. The linear chain structure in PLA results in low melt strength, sagging, and necking which limits its processing [3]. Thus, the considerable efforts have been directed to overcome the weaknesses in PLA polymer. Several studies have focused on incorporating the bio-based nanofillers such as cellulose fibrils, fibers and nanocrystals to strengthen PLA [4,5].

Cellulose nanocrystals (CNCs) have attracted a huge attention as reinforcing agent in polymeric matrices. CNCs are cellulose-based, non-toxic, and biodegradable nanoparticles isolated from bulk cellulose of woody and non-woody plants [6]. The high mechanical and barrier properties in CNCs suggest the competitive potential for the application as reinforcing agent in polymeric materials [7]. It has been observed that the optimal performance of CNCs as reinforcing agent in polymeric matrix is ascribed by the dispersion quality of CNCs through polymeric matrix. For optimal improvement, uniform dispersion of CNCs in polymers is required [8].

Rheological properties in composite materials play a significant role in improving the processability of composites as the processing operation such as extrusion and injection molding involve high shear rates [9]. Cellulose nanocrystals have been reported to be a good rheological modifier for different polymers because they surround themselves between polymer chains, providing high stability to the polymer network [10]. A significant change in the melting behavior and rheological properties of nanocomposites has been observed by the incorporation of nanofillers [11,12]. Musa et al. studied the effects of incorporating

* Corresponding author.
E-mail address: Jamileh.shojaeiarani@ndsu.edu (J. Shojaeiarani).

https://doi.org/10.1016/j.compositesb.2018.12.128
Received 14 May 2018; Received in revised form 17 December 2018; Accepted 30 December 2018
Available online 31 December 2018
1359-8368/

CNCs on the rheological behavior of nanocomposites. They found that the high interfacial area resulting from inter-particle interactions governs the rheological properties of nanocomposites [7].

Different studies have shown that well-dispersed CNCs can enhance the performance characteristics of PLA through improvement in the level of crystallinity and formation of matrix-nanofiller network [13]. Therefore, improving the CNCs dispersion in PLA has been extensively explored though different chemical surface modification techniques and mechanical processing [9,14,15].

It was reported that the application of masterbatch approach can enhance the dispersion quality of CNCs in host polymer [15]. The highly concentrated masterbatches are diluted using extrusion process considering the let-down ratio or mixing ratio (masterbatches: polymer ratio) [15]. The time-intensive film casting is the most commonly used technique in preparing masterbatches [9]. Long time drying process in film casting process favored the formation of micro-sized CNC aggregates through polymer matrix [15]. Spin-coating is a newly introduced method for fabricating highly concentrated masterbatches. The short drying time in spin-coating deposition technique hindered the formation of CNCs aggregates in polymer matrix [15].

In this study, the impact of two different masterbatch preparation methods on the molecular structure, rheological, viscoelastic, and thermal properties of nanocomposites were evaluated. Nanocomposites were manufactured by diluting film casted and spin-coated masterbatches via melt compounding followed by injection molding process. The modified CNCs were prepared using poly(ethylene oxide) through physical attachment method.

2. Experimental

2.1. Materials

Poly(lactic acid) grade 2003D manufactured by Nature Works LLC (Minnetonka, MN, USA) with the glass transition of 55–60 °C and melt flow of 6 g/10 min was used as a biopolymer. USDA-Forest Service, Forest Products Laboratory (Madison, WI, USA) provided cellulose nanocrystals (CNCs) with dimensions of 10–15 nm. Analytical grade chloroform manufactured by Sigma-Aldrich (St. Louis, MO, USA) was used in this study. Polyethylene oxide (PEO) with the molecular number of 10^6 g mol^{-1} and a purity of 99% was obtained from Sigma-Aldrich (St. Louis, MO, USA).

2.2. Surface modification treatment

CNCs were treated using poly(ethylene oxide) to decrease the hydrophilicity character of CNCs and to enhance the compatibility between CNCs and PLA matrix. An aqueous suspension of CNCs (4 wt%) and a suspension of PEO (1 wt%) were separately prepared and then were mixed together with the ratio of 4:1 (CNCs: PEO). The freeze-dried mixture was used as modified CNCs (p-CNCs) [16,17].

2.3. Scanning electron microscopy of masterbatches

The formation of CNC aggregates through the thickness of the thin film masterbatches were studied through scanning electron microscopy (SEM) images. A JSM-7600F scanning electron microscopy (USA Inc., Peabody, MA, USA) operating at 10, and 15 kV was used to take the images with different magnification factors (150, 200, 500, and 1000 ×).

2.4. Scanning electron microscopy (SEM) of composites

The morphology of the nanocomposite samples was examined using a scanning electron microscope (SEM, JSM-6010LA, Peabody, MA, USA). The impact-fractured surface of nanocomposites was recorded at an accelerating voltage of 10.0 kV and a magnification of 200 × . The fractured surfaces were coated with a thin layer of conductive carbon prior to examining by SEM to avoid samples charging.

Table 1
Composition of the nanocomposite materials.

Materials code	Composition		Methods
	PLA (wt%)	p-CNCs (wt%)	
PLA	100	0	–
F-PLA1	99	1	Film casting
F-PLA3	97	3	Film casting
F-PLA5	95	5	Film casting
S-PLA1	99	1	Spin-coating
S-PLA3	97	3	Spin-coating
S-PLA5	95	5	Spin-coating

2.5. Preparation of nanocomposites

Film casting and spin-coating methods were used to prepare highly concentrated CNCs masterbatches (15 wt%), following the method which was reported in the previous work [15]. The nanocomposites with different p-CNCs contents (1%, 3%, and 5%) were prepared using a co-rotating twin-screw extruder (Leistritz, Mic 18/GL-40D, Somerville, NJ, USA) and injection-molding machine (Technoplas Inc. SIM-5080). Prior to injection molding, the extruded pellets were placed in an oven (Binder ED, Bohemia, NY, USA) for 24 h at 60 °C to remove the excess moisture from the pellets. Table 1 shows the processing condition and material codifications used in this study.

2.6. Gel permeation chromatography

The weight average molecular weight (M_w) and the number average molecular weight (M_n) were measured using a gel permeation chromatography (EcoSEC HLC-8320GPC, Tosoh Bioscience, Japan) equipped with a differential refractometer (DRI) detector. Nanocomposite solutions (1 mg/ml) were prepared in tetrahydrofuran solvent and filtered using filter disk (0.2 μm pore size) prior the testing. The column temperature was maintained at 40 °C, and the solvent flow rate was set at 0.35 ml/min.

2.7. Dynamic mechanical analysis

Dynamic mechanical analysis was used to study the molecular relaxation behavior of PLA and nanocomposites. Measurements were recorded using a DMA Q800 (TA Instruments, New Castle, DE, USA) following ASTM D4065 standard procedure [18]. Data were recorded in the temperature range of 25–90 °C with a scanning rate of 1 °C/min, and a fixed frequency of 1 Hz in a dual cantilever mode. The storage modulus and tan δ as a function of temperature were reported.

2.8. Rheological properties

The flow properties (rheological properties) of materials were measured using a Rheometer AR 2000 (TA Instruments, New Castle, DE, USA). The rheological properties of PLA and nanocomposites were measured in an oscillatory mode. The sample weighing 5 gr was placed between two parallel plates with 25 mm diameter and a gap of 1 mm at 170 °C. Prior to testing, samples were dried in a vacuum oven set at 65 °C for 8 h to avoid a significant decline in viscosity as a result of moisture uptake in the samples.

2.9. Thermogravimetric analysis (TGA)

Thermal stability of pure PLA and nanocomposites were studied using thermogravimetric analyzer Q500 (TA, New Castle, DE, USA). A

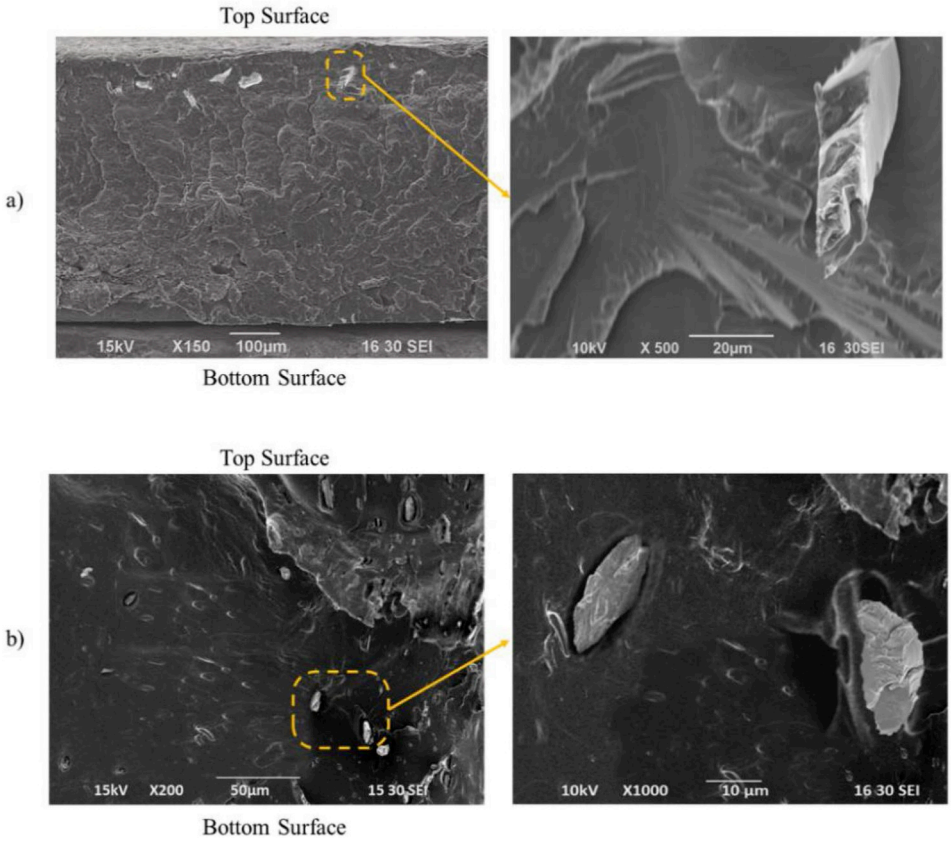

Fig. 1. The comparison of CNCs aggregates formation in the masterbatches at different magnification factors: a) solvent cast, b) spin-coated.

5–7 mg of each formulation was placed in an aluminum pan and temperature range was set in the range of 25–600 °C with a scanning rate of 10 °C/min. The corresponding TGA and derivative thermogravimetry (DTG) curves were recorded.

3. Results and discussion

3.1. Scanning electron microscopy of masterbatches

The distribution of CNC aggregates through the thickness of the highly concentrated thin film masterbatches were studied and Fig. 1 illustrates the dispersion quality and size of CNC aggregates in the masterbatches.

The individual CNCs are hardly distinguishable, however, the presence of CNC aggregates (spotted by arrows) can be observed for both set of samples (i.e. solvent cast and spin coated masterbatches). Due to the relatively low evaporation rate in the solvent cast masterbatch, the concentration of CNCs varies vertically along with the thickness of the masterbatch and the highest concentration of CNC aggregates happens close to the top surface (free surface) of the film (Fig. 1a). However, in the spin-coated masterbatch, the CNC aggregates are scattered throughout the masterbatch thickness (Fig. 1b). These observations confirm the lower CNCs mobility in the spin-coated masterbatch as a result of high evaporation rate of the solvent as well as the centrifugal force generated from rotating substrate [15]. In fact, the dispersion of CNCs can lower their free energy through doing self-assembly and forming clusters [19]. During time-intensive solvent evaporation process in solvent casting method, solvent molecules exclude the CNCs molecules and assist in drawing the CNCs closer. This allows for the formation of CNC aggregates with relatively larger size in comparison with time-efficient solvent evaporation in spin-coated thin films.

3.2. Scanning electron microscopy (SEM) of nanocomposites

SEM was used to get an insight into nanocomposite structures [20], and the corresponding images are illustrated in Fig. 2. The CNCs in the nanocomposites prepared using spin-coated method (S-PLA) appeared to be uniformly distributed through PLA matrix, however the formation of CNC aggregates in F-PLA nanocomposites further confirmed the poor dispersion of CNC in solvent cast masterbatches (Fig. 1a).

The formed CNC aggregates in highly concentrated masterbatches due to increasing probability of adjacent hydroxyl moieties of CNCs [21] led to the poor CNC dispersion in solvent cast samples. The improvement of the dispersion can be ascribed to the excellent compatibility between PLA and CNCs [22] particularly at low CNC contents (1 and 3% wt).

3.3. Gel permeation chromatography

The number average molecular weight (M_n) and the weight average molecular weight (M_w) are two important properties in polymers, which influence different behaviors such as melt viscosity, mechanical properties and processability. PLA with linear chain is so sensitive to manufacturing processes, revealing a rapid reduction in M_n and M_w as a result of thermal degradation under high shear [23,24]. A significant decline in the molecular weight of PLA was reported in different studies due to the addition of different nanofillers [25–27]. Table 2 shows the values of M_w, M_n and dispersity index (M_w/M_n) of PLA and nanocomposites after extrusion process.

All nanocomposites exhibited a decline in M_w, M_n as compared to pure PLA, suggesting the presence of p-CNCs provoked the degradation of PLA during composite preparation, and the drop was linearly correlated to the nanofillers loadings. The observed results were in good agreement with another study, reporting PLA chain degradation due to the incorporating the nanofillers [28].

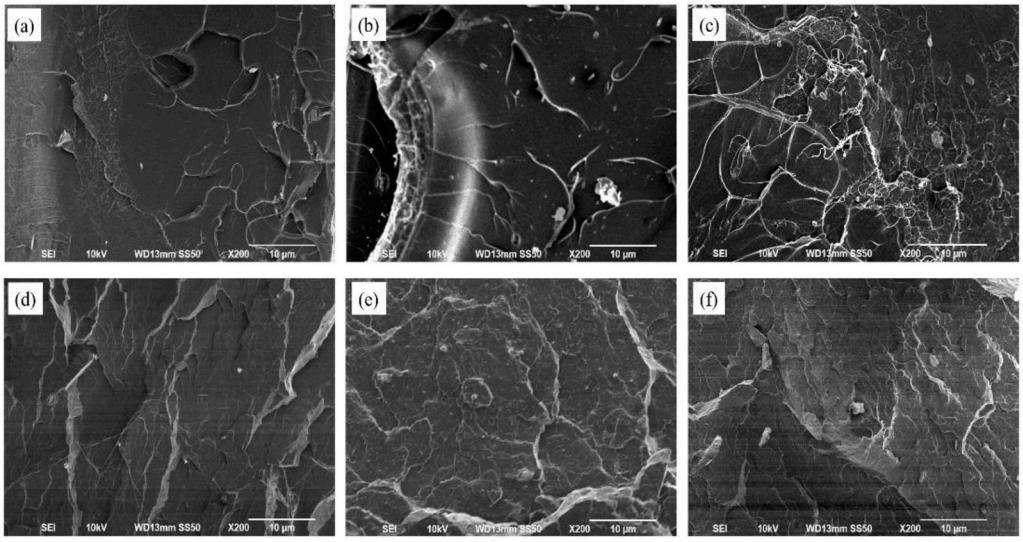

Fig. 2. The SEM micrographs of fracture surface of PLA-CNC nanocomposites: a) F-PLA1, b) F-PLA3, c) F-PLA5, d) S-PLA1, e) S-PLA3 and f) S-PLA5.

The number average molecular weight (M_n) refers to the colligative properties of polymers and the spin-coated nanocomposites exhibited lower M_n as compared to film cast samples. It was reported that polymer chain cleavage can happen when heat or high pressure are generated during processing [29]. The lower M_n in spin-coated nanocomposites can likely be attributed to the high pressure caused by injection during the masterbatch preparation technique, which interrupted molecular chains. In addition, it has been claimed that the presence of residual solvent in the samples could result in a decrease in M_n of polymers [24]. Due to the short drying time in the spin-coating method, the solvent did not evaporate completely, and some residual solvent was trapped in the masterbatches. The amount of residual solvent in each masterbatches before feeding into extruder was found to be 8.65 wt% and 1.37 wt% in spin-coated and film cast masterbatches, respectively. Therefore, the lower M_n in spin-coated samples could probably be a result of both the higher residual solvent in spin-coated masterbatches and the high injection pressure during spin-coated masterbatch preparation process.

Higher M_w was observed in spin-coated samples in comparison with their film cast counterparts. This observation suggested that the M_w favored spin-coating method. The higher M_w in spin-coated nanocomposites can be attributed to the strong interactions between PLA and CNCs. In general, the higher the molecular weight, the greater the degree of chain entanglement [30].

The dispersity index (DI) or heterogeneity index is a ratio of M_w to M_n, measuring the distribution of molecular mass in a polymer. Polymers with higher DI have wider molecular weight distribution. The dispersity index depends on the reaction condition and manufacturing process. It strongly affects polymer performance and the processing characteristics [31]. In general, polymers with lower DI are difficult to process as the shear-thinning tendency is low. However, polymeric materials with broader molecular weight distribution tend to thin at lower temperatures and make molding and extrusion process easier. In spin-coated samples, DI constantly increased with p-CNC loading level. However, film cast samples exhibited narrower DI. The shorter polymer length for the higher molecular weight can be considered a result of high injection pressure in spin-coating masterbatch preparation technique.

Table 2
The average molecular weight, the average molecular number, and the dispersity index (DI) of samples.

Materials code	M_n[a] (g/mol)	M_w (g/mol)	DI
PLA	97245	202517	2.08
F-PLA1	95081	193776	2.03
F-PLA3	83444	144434	1.73
F-PLA5	82423	137880	1.67
S-PLA1	94148	201791	2.14
S-PLA3	57226	183241	3.20
S-PLA5	52532	170335	3.24

[a] M_n: Number average molecular weight and M_w: Weight average molecular weight.

3.4. Dynamic mechanical analysis (DMA)

The viscoelastic properties of polymers are strongly associated with the molecular structure and molecular relaxation motion. The viscoelastic properties of nanocomposites directly govern the load bearing capability of materials and attribute towards the interfacial bonding between matrix and nanofillers.

The storage modulus of PLA and nanocomposites at two different temperatures in glassy and rubbery states are shown in Table 3. It can be observed that all the composite samples exhibited higher storage modulus in comparison with PLA in the glassy state. The improved storage modulus in nanocomposites can be attributed to the growth in the stiffness of the PLA matrix owing to reinforcing effect imparted by p-CNCs that led to a greater degree of stress transfer at the PLA-p-CNCs interface. Particularly, the spin-coated nanocomposites reinforced with 1 wt% and 3 wt% p-CNCs exhibited higher storage modulus in the glassy and rubbery states in comparison with film cast samples. It is reported that a slight decrease in storage modulus in S-PLA5 is associated with the presence of residual solvent [15].

Table 3
The viscoelastic properties in PLA and nanocomposites.

Materials	Storage modulus (MPa)		T_g (°C)	Tan δ peak intensity
	35 °C	85 °C		
PLA	2001.2 ± 4.0	7.01 ± 0.2	65.16 ± 1.5	2.72 ± 0.02
F-PLA1	2500.4 ± 5.2	9.09 ± 0.1	65.92 ± 1.6	1.83 ± 0.06
F-PLA3	2397 ± 6.3	5.43 ± 0.1	67.8 ± 1.2	2.65 ± 0.01
F-PLA5	2300.3 ± 10.7	10.46 ± 0.1	65.99 ± 2.0	1.78 ± 0.03
S-PLA1	2849.4 ± 6.1	14.68 ± 0.2	65.18 ± 1.3	2.23 ± 0.04
S-PLA3	2467.9 ± 2.6 … 36	7.41 ± 0.1	67.05 ± 0.8	2.57 ± 0.03
S-PLA5	2056.4 ± 3.5	8.54 ± 0.1	65.71 ± 1.2	1.96 ± 0.04

The better interaction between matrix and nanofillers provides a clear explanation for the increase in storage modulus with increasing M_w in spin-coated nanocomposites. In general, polymers with low M_w possess low number of long flexible chains. The lack of long flexible chain in the polymers would decrease the strength and elastic modulus in polymer materials [32]. In this work, S-PLA1 with highest M_w among nanocomposites (Table 2) and better dispersed network (Fig. 2) exhibited the highest storage modulus followed by F-PLA1 in glassy state.

Tan δ curve is associated with the segmental motion in molecular chains. The position of tan δ peak reveals the glass transition temperature (T_g) in polymeric materials [33,34]. The glass transition temperature of PLA and nanocomposites are shown in Table 3. The incorporation of p-CNCs into PLA slightly increased T_g. As expected from Flory-Fox equation (Eq. (1)), the spin-coated nanocomposites with smaller M_n exhibited lower T_g than film cast samples [35] (Table 2).

$$T_g = T_{g\infty} - \frac{K}{M_n} \quad \text{Eq. 1}$$

In which, T_g is glass transition and $T_{g\infty}$ reveals the maximum glass transition temperature occurs theoretically for the polymer with an infinite molecular weight. K is an empirical constant and associated with the free volume in the polymer chains.

The lower glass T_g in spin-coated nanocomposites can be attributed to more freedom in molecular mobility in spin-coated PLA-CNC. In general, the polymers with lower M_n possess more free volume at the end of each polymer chain and this, in turn, leads to higher chain mobility. In another word, slightly higher T_g in film cast samples can be related to the decreased mobility of the matrix chain, due to the higher M_n in film cast samples.

The intensity of tan δ indicates the mobility of polymer chain segments at the corresponding temperature [36]. In addition, the way in which the materials absorb or disperse the energy during deformation can be observed from tan δ intensity. A higher tan δ intensity indicates that more energy is dissipated, and the material exhibits more viscous behavior. However, the lower tan δ value points out the behavior that is more elastic. The tan δ peak value decreased in all composite samples as compared to pure PLA, owing to the presence of p-CNCs. This observation was probably due to the decrease in the mobility of the polymer molecular chains as restricted by p-CNCs. As expected, spin-coated nanocomposites exhibited higher tan δ peak value in comparison with film cast samples. This observation was in good agreement with smaller M_n in spin-coated samples (Table 2).

3.5. Thermogravimetric analysis (TGA)

Thermal stability of samples was studied through weight loss and the corresponding derivative curves (DTG) (Fig. 3). Thermal properties of PLA and nanocomposites including initial decomposition temperature (T_{onset}), decomposition temperature at 50% weight loss (T_{50}), maximum decomposition (T_{peak}), and final degradation temperatures (T_{endset}) are reported in Table 4.

Table 4
Thermal properties of PLA and PLA-PCNCs nanocomposites.

Sample code	T_{onset} (°C)	$T_{50\,wt\%}$ (°C)	T_{peak} (°C)	T_{endset} (°C)	Weight loss (%)
PLA	301.13	328.34	332.24	380.39	99.73
F-PLA1	311.22	359.37	345.32	397.72	99.37
F-PLA3	319.18	358.86	344.8	402.89	99.47
F-PLA5	310.72	358.05	345.24	395.71	99.61
S-PLA1	335.72	399.65	375.25	400.62	99.43
S-PLA3	316.30	355.07	372.1	385.72	99.54
S-PLA5	314.18	357.82	370.82	395.04	99.37

The thermal stability of PLA matrix was improved by addition of p-CNCs, confirming an increase in both the onset and endset degradation temperatures. This behavior can be tied to a barrier effect of the PEO coated CNCs towards polymer decomposition as has been reported by Azouz et al. [16]. Particularly, the relatively higher thermal stability in spin-coated nanocomposites reinforced by 1 wt% CNCs can be attributed to the formation of greater intermolecular interaction in composite structure as supported by higher M_w and uniform dispersion of CNCs through *PLA* matrix (Fig. 2d). The alignment of molecular chains due to high pressure in the injection process in spin-coating method can induce the formation of network-like connections between composite components. The more stable structure [37] in spin-coated samples as a result of more uniform dispersion of CNCs (Fig. 2) can hinder the thermal decomposition at elevated temperatures.

Considering the weight loss profiles for pure PLA and PLA nanocomposites (Fig. 3), thermal decomposition of all samples except S-PLA5 happened in a typical one-step degradation pattern. The observation of one step degradation suggested the simultaneous degradation in all components [38]. The presence of two separate peaks in S-PLA5 might be a result of incorporating high amount of CNCs and the corresponding non-uniform dispersion as shown in previous study [15].

The total mass loss values for the nanocomposites containing modified CNCs are slightly lower than pure PLA. However, no significant change in the char yield was observed for PLA composite samples as compared with pure PLA.

3.6. Rheological properties

The dynamic oscillatory shear measurements were carried out to study the response of PLA and PLA-CNC nanocomposites to the dynamic shearing. Fig. 4 depicts a representative curve for complex viscosity in PLA and nanocomposites. The complex viscosity of pure PLA and nanocomposite samples decreased with increasing frequency,

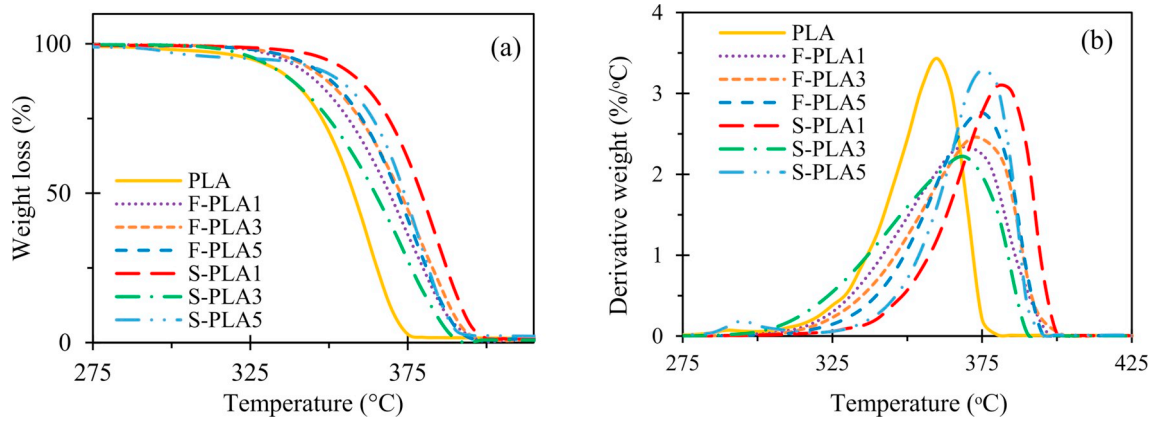

Fig. 3. Representative thermogravimetric (TGA) and Derivative (DTG) thermograms of pure PLA and nanocomposites.

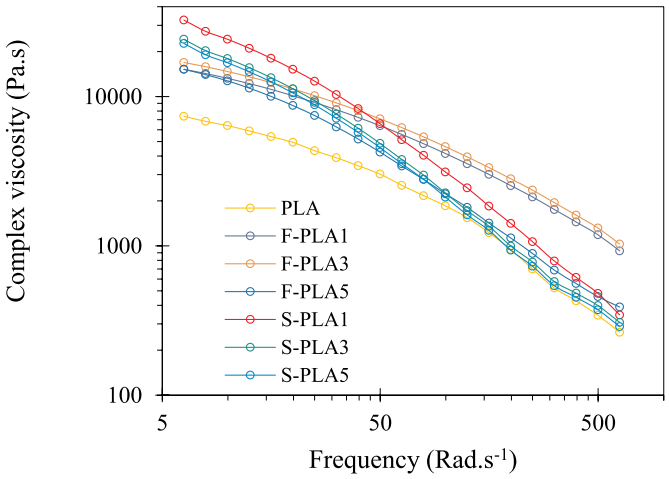

Fig. 4. Complex viscosity for PLA and nanocomposites.

exhibiting non-Newtonian behavior.

The addition of p-CNCs into PLA through both masterbatch preparation routes increased the melt strength of nanocomposites. This behavior indicates the formation of interconnected network-like structure in the composite samples because of the interaction between matrix and nanofillers. A similar observation was reported by Kamal et al. (2015), in which a significant improvement in complex viscosity was reported by the addition of CNCs into PLA matrix [7]. The high viscosity of nanocomposites was caused by the flow restrictions of PLA chains in the molten state due to the presence of p-CNCs. The polymer chain structure significantly governs the rheological properties and the processability of the polymer.

The molten viscosity and the molecular weight of polymers are correlated to each other based on Mark-Houwink equation (Eq. (2)) [39].

$$[\eta] = KM_w^a \qquad \text{Eq. 2}$$

Where a and K are Mark-Houwink constants and depend on the nature of polymer and solvent.

The higher viscosity in S-PLA1 was attributed to the higher M_w. All samples exhibited shear-thinning behavior, which was more predominant in spin-coated nanocomposites. The shear thinning behavior in polymers is associated with the disentanglement of polymer chains during flow. The onset of shear thinning in polymers is the point, in which, the rate of externally applied movement overcomes the rate of formation of entanglements in polymer chains. In shear thinning phenomenon, the crosslink density of the network decreases, resulting in a decline in the viscosity [40]. The samples with higher M_w experienced more disentanglement during flow at higher shear rate, exhibiting more tendency for shear thinning at higher frequencies. Shear thinning in spin-coated samples could speed up the polymer flow and decrease heat generation and energy consumption through processing [41].

Network structure of PLA and nanocomposites was also studied through storage and loss moduli as a function of angular frequency at 170 °C (Fig. 5). The storage modulus increased with increasing the angular frequency, but the rate of increment in modulus reduced as the frequency increased.

In general, at lower frequencies, the interactions between PLA and p-CNCs overcome the applied shear. However, at higher frequencies, the interfacial bonding between PLA and p-CNCs cannot resist the external shear. This in turn, can result in a reduction in the slope of storage modulus. The storage modulus in PLA exhibited an improvement upon addition of p-CNCs, submitting the formation of interfacial bonding between PLA and p-CNCs, which led to more stress transfer from matrix to nanofillers. In particular, the highest storage modulus was observed in S-PLA1 followed by F-PLA1. This observation was in good agreement with an earlier reported study, in which, polymer with higher molecular weight exhibited higher storage modulus [42]. However, the lower storage modulus in PLA was probably due to the reduction in molecular entanglements in the pure PLA over the high frequency rate.

The loss modulus of PLA and nanocomposites exhibited a trend like storage modulus at different p-CNC contents (Fig. 5b); however, the deviation from pure PLA was more pronounced in loss modulus. The incorporation of p-CNCs in PLA resulted in a substantial increase in the loss modulus, indicating a further increased entanglement density in PLA-CNC nanocomposites in comparison with pure PLA. These observations are in good agreement with the results reported by Hassan et al. They observed a similar trend in storage and loss modulus of PLA and PLA blends with increasing frequency [43]. In addition, all samples exhibited higher storage modulus than loss modulus over the entire range of frequency. This was an indication of the dominance of solid-like relaxation behavior, typically found in strong gels [44].

4. Conclusion

PLA-p-CNC nanocomposites were prepared through diluting masterbatches of film casted and spin-coated films, using melt compounding followed by injection molding. The molecular structure, dynamic mechanical, thermal stability, and rheological properties of PLA and nanocomposites were studied. The GPC results suggested that the samples prepared using spin-coating method exhibited higher molecular weight with a wide distribution of chain lengths. This observation could probably be due to high injection pressure during spin-coated masterbatch preparation process. The viscoelastic and rheological

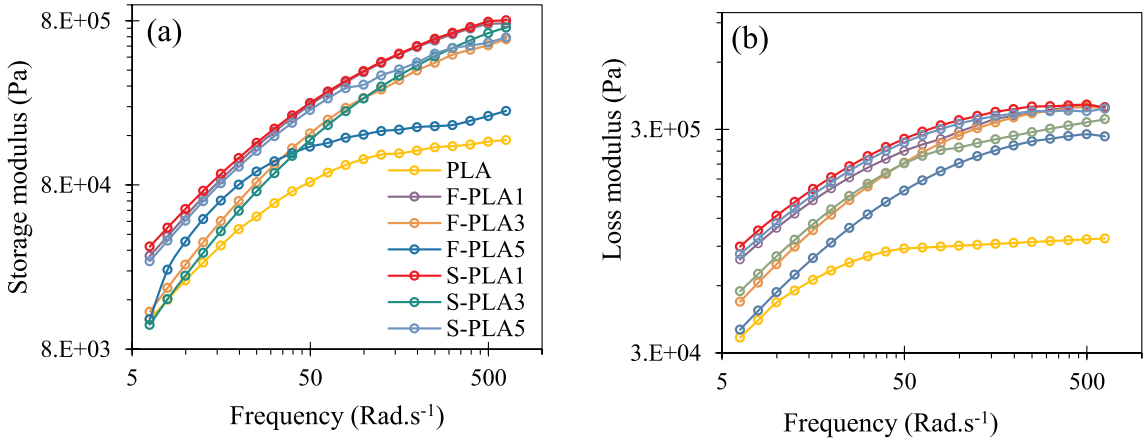

Fig. 5. (a) Storage modulus and (b) loss modulus as a function of frequency of PLA and nanocomposites.

properties of the nanocomposites demonstrated a close relationship with the number average molecular weight and the weight average molecular weight. The addition of p-CNCs into PLA resulted in an improvement in storage modulus as p-CNCs imparted reinforcing effect on the nanocomposites. The spin-coated nanocomposites with higher molecular number had higher storage modulus as compared to their film cast counterpart. This study shows that PLA nanocomposite characteristics can be engineered through different mechanical processing technique and the spin-coating method is a promising approach for masterbatch preparation method to improve the properties of the PLA-CNC nanocomposites.

Acknowledgment

The authors would like to acknowledge National Science Foundation (NSF), ND EPSCoR (grant No.11A1355466) for supporting this research.

Appendix A. Supplementary data

Supplementary data to this article can be found online at https://doi.org/10.1016/j.compositesb.2018.12.128.

References

[1] Plackett DV, Holm VK, Johansen P, Ndoni S, Nielsen PV, Sipilainen-Malm T, et al. Characterization of l-polylactide and l-polylactide–polycaprolactone co-polymer films for use in cheese-packaging applications. Packag Technol Sci 2006;19(1):1–24.
[2] Al-Itry R, Lamnawar K, Maazouz A. Reactive extrusion of PLA, PBAT with a multifunctional epoxide: physico-chemical and rheological properties. Eur Polym J 2014;58:90–102.
[3] Hernández-Alamilla M, Valadez-Gonzalez A. The effect of two commercial melt strength enhancer additives on the thermal, rheological and morphological properties of polylactide. J Polym Eng 2016;36(1):31–41.
[4] Espino-Pérez E, Bras J, Almeida G, Plessis C, Belgacem N, Perré P, et al. Designed cellulose nanocrystal surface properties for improving barrier properties in polylactide nanocomposites. Carbohydr Polym 2018;183:267–77.
[5] Huan S, Liu G, Cheng W, Han G, Bai L. Electrospun poly (lactic acid)-based fibrous nanocomposite reinforced by cellulose nanocrystals: impact of fiber uniaxial alignment on microstructure and mechanical properties. Biomacromolecules; 2018.
[6] George J, Sabapathi S. Cellulose nanocrystals: synthesis, functional properties, and applications. Nanotechnol Sci Appl 2015;8:45.
[7] Kamal MR, Khoshkava V. Effect of cellulose nanocrystals (CNC) on rheological and mechanical properties and crystallization behavior of PLA/CNC nanocomposites. Carbohydr Polym 2015;123:105–14.
[8] López de Dicastillo C, Garrido L, Alvarado N, Romero J, Palma JL, Galotto MJ. Improvement of polylactide properties through cellulose nanocrystals embedded in poly (vinyl alcohol). Electrospun Nanofibers. Nanomaterials 2017;7(5):106.
[9] Fortunati E, Yang W, Luzi F, Kenny J, Torre L, Puglia D. Lignocellulosic nanostructures as reinforcement in extruded and solvent casted polymeric nanocomposites: an overview. Eur Polym J 2016;80:295–316.
[10] Ching YC, Ali ME, Abdullah LC, Choo KW, Kuan YC, Julaihi SJ, et al. Rheological properties of cellulose nanocrystal-embedded polymer composites: a review. Cellulose 2016;23(2):1011–30.
[11] Majid M, Hassan E-D, Davoud A, Saman M. A study on the effect of nano-ZnO on rheological and dynamic mechanical properties of polypropylene: experiments and models. Compos B Eng 2011;42(7):2038–46.
[12] Gupta A, Simmons W, Schueneman GT, Hylton D, Mintz EA. Rheological and thermo-mechanical properties of poly (lactic acid)/lignin-coated cellulose nanocrystal composites. ACS Sustainable Chem Eng 2017;5(2):1711–20.
[13] Bagheriasl D, Carreau PJ, Riedl B, Dubois C, Hamad WY. Shear rheology of polylactide (PLA)–cellulose nanocrystal (CNC) nanocomposites. Cellulose 2016;23(3):1885–97.
[14] Shojaeiarani J, Bajwa DS, Stark NM. Green esterification: a new approach to improve thermal and mechanical properties of poly(lactic acid) composites reinforced by cellulose nanocrystals. J Appl Polym Sci 2018;135(27):46468.
[15] Shojaeiarani J, Bajwa D, Stark N. Spin-coating: a new approach for improving dispersion of cellulose nanocrytals and mechanical properties of poly(lactic acid) composites. Carbohydrate polymers; 2018.
[16] Ben Azouz K, Ramires EC, Van den Fonteyne W, El Kissi N, Dufresne A. Simple method for the melt extrusion of a cellulose nanocrystal reinforced hydrophobic polymer. ACS Macro Lett 2011;1(1):236–40.
[17] Huang J, Chen Y, Chang PR. Surface ModIfIcatIon of celluloSe nanocryStalS for nanocoMpoSIteS. Surf Modif Biopolym 2015:258.
[18] ASTM DI. Standard practice for plastics: dynamic mechanical properties: determination and report of procedures. ASTM International; 2012.
[19] Sau TK, Murphy CJ. Self-assembly patterns formed upon solvent evaporation of aqueous cetyltrimethylammonium bromide-coated gold nanoparticles of various shapes. Langmuir 2005;21(7):2923–9.
[20] Wang W, Kan Y, Liu J, Liew KM, Liu L, Hu Y. Self-assembly of zinc hydroxystannate on amorphous hydrous TiO2 solid sphere for enhancing fire safety of epoxy resin. J Hazard Mater 2017;340:263–71.
[21] Nicharat A, Sapkota J, Foster EJ. Pre-mixing and masterbatch approaches for reinforcing poly (vinyl acetate) with cellulose based fillers. Ind Crop Prod 2016;93:244–50.
[22] Wang W, Kan Y, Pan H, Pan Y, Li B, Liew K, et al. Phosphorylated cellulose applied for the exfoliation of LDH: an advanced reinforcement for polyvinyl alcohol. Compos Appl Sci Manuf 2017;94:170–7.
[23] Chávez-Montes WM, González-Sánchez G, López-Martínez EI, de Lira-Gómez P, Ballinas-Casarrubias L, Flores-Gallardo S. Effect of artificial weathering on PLA/nanocomposite molecular weight distribution. Polymers 2015;7(4):760–76.
[24] Murariu M, Bonnaud L, Yoann P, Fontaine G, Bourbigot S, Dubois P. New trends in polylactide (PLA)-based materials:“Green” PLA–Calcium sulfate (nano) composites tailored with flame retardant properties. Polym Degrad Stabil 2010;95(3):374–81.
[25] Zaidi L, Kaci M, Bruzaud S, Bourmaud A, Grohens Y. Effect of natural weather on the structure and properties of polylactide/Cloisite 30B nanocomposites. Polym Degrad Stabil 2010;95(9):1751–8.
[26] Fujimoto Y, Ray SS, Okamoto M, Ogami A, Yamada K, Ueda K. Well-controlled biodegradable nanocomposite foams: from microcellular to nanocellular. Macromol Rapid Commun 2003;24(7):457–61.
[27] Ray SS, Okamoto M. Biodegradable polylactide and its nanocomposites: opening a new dimension for plastics and composites. Macromol Rapid Commun 2003;24(14):815–40.
[28] Fukushima K, Tabuani D, Abbate C, Arena M, Ferreri L. Effect of sepiolite on the biodegradation of poly (lactic acid) and polycaprolactone. Polym Degrad Stabil 2010;95(10):2049–56.
[29] King K. Changes in the functional properties and molecular weight of sodium alginate following γ irradiation. Food Hydrocolloids 1994;8(2):83–96.
[30] Karak N. Fundamentals of polymers: raw materials to finish products. PHI Learning Pvt. Ltd.; 2009.
[31] Panzer F, Bässler H, Lohwasser R, Thelakkat M, Köhler A. The impact of polydispersity and molecular weight on the order–disorder transition in poly (3-hexylthiophene). J Phys Chem Lett 2014;5(15):2742–7.
[32] Crosby AJ, Lee JY. Polymer nanocomposites: the “nano” effect on mechanical properties. Polym Rev 2007;47(2):217–29.
[33] Pinheiro A, Mano JF. Study of the glass transition on viscous-forming and powder materials using dynamic mechanical analysis. Polym Test 2009;28(1):89–95.
[34] Priya L, Jog J. Poly (vinylidene fluoride)/clay nanocomposites prepared by melt intercalation: crystallization and dynamic mechanical behavior studies. J Polym Sci B Polym Phys 2002;40(15):1682–9.
[35] Fox TG, Flory PJ. The glass temperature and related properties of polystyrene. Influence of molecular weight. J Polym Sci Polym Chem 1954;14(75):315–9.
[36] Hill D, Perera M, Pomery P, Toh H. Dynamic mechanical properties of networks prepared from siloxane modified divinyl benzene pre-polymers. Polymer 2000;41(26):9131–7.
[37] Poletto M, Pistor V, Zattera AJ. Structural characteristics and thermal properties of native cellulose. Cellulose-fundamental aspects. InTech; 2013.
[38] Kucharczyk P, Pavelková A, Stloukal P, Sedlarík V. Degradation behaviour of PLA-based polyesterurethanes under abiotic and biotic environments. Polym Degrad Stabil 2016;129:222–30.
[39] Wang J, Huang H, Huang X. Molecular weight and the Mark-Houwink relation for ultra-high molecular weight charged polyacrylamide determined using automatic batch mode multi-angle light scattering. J Appl Polym Sci 2016;133(31).
[40] Morris E, Cutler A, Ross-Murphy S, Rees D, Price J. Concentration and shear rate dependence of viscosity in random coil polysaccharide solutions. Carbohydr Polym 1981;1(1):5–21.
[41] Franck A. Understanding rheology of thermoplastic polymers. TA Instruments 2004;118:1–8.
[42] Cooper-White JJ, Mackay ME. Rheological properties of poly (lactides). Effect of molecular weight and temperature on the viscoelasticity of poly (l-lactic acid). J Polym Sci B Polym Phys 1999;37(15):1803–14.
[43] Hassan E, Wei Y, Jiao H, Muhuo Y. Dynamic mechanical properties and thermal stability of poly (lactic acid) and poly (butylene succinate) blends composites. J Fiber Bioeng Inf 2013;6(1):85–94.
[44] Le Pluart L, Duchet J, Sautereau H, Halley P, Gerard J-F. Rheological properties of organoclay suspensions in epoxy network precursors. Appl Clay Sci 2004;25(3–4):207–19.